Low-frequency impedance of quantized Hall conductors

W. Desrat, D. K. Maude, L. B. Rigal, M. Potemski, and J. C. Portal
Grenoble High Magnetic Field Laboratory, Max Planck Institut für Festkörperforschung and Centre National de la Recherche Scientifique, BP 166, 38042 Grenoble Cedex 9, France

L. Eaves and M. Henini
Department of Physics, University of Nottingham, Nottingham, NG7 2RG, United Kingdom

Z. R. Wasilewski
Institute for Microstructural Sciences, National Research Council, Ottawa, Canada, K1A 0R6

A. Toropov
Institute of Semiconductor Physics, Russian Academy of Sciences, Siberian Division, Novossibirsk 630090 Russia

G. Hill and M. A. Pate
Department of Electronic and Electrical Engineering, University of Sheffield, Sheffield S1 4DU, United Kingdom
(Received 19 May 2000)

The longitudinal and the Hall impedances have been measured as a function of the frequency in a two-dimensional electron gas at low temperatures. The frequency dependence of the longitudinal impedance can be explained in terms of an equivalent parallel LCR circuit. An effective inductance term arises due to the capacitive coupling between edge states and is shown to scale as $1/\nu^2$ for different filling factors. In the low-frequency range the relative difference between the ac and dc values of the Hall impedance is found to depend quadratically on the frequency and to scale as $1/\nu^3$. These results are shown to be consistent with the existing theoretical model based on the edge-state picture. Finally, the observed symmetry relations when exchanging current contacts or reversing magnetic field are discussed.

I. INTRODUCTION

The transport properties of a two-dimensional electron gas (2DEG) have been extensively investigated, leading notably to the discovery of the integer and fractional quantum Hall effects.[1,2] Typical transport measurements are carried out under quasi-dc conditions with a low-frequency ($\sim$10 Hz) alternating current in the range 1–100 nA. Microwave frequencies have been employed to study edge magnetoplasmons[3–6] and finite-frequency scaling.[7,8] Low-frequency (0–10 kHz) measurements have concentrated on the small deviation of the quantized Hall resistance from the dc value[9] with a view to defining a new ac resistance standard[10] and to investigations involving a capacitively coupled gate[11,12] or inductive probing of edge state transport.[13]

In this paper, we present the frequency dependence (0–50 kHz) of the longitudinal impedance Z_{xx} and the Hall impedance Z_{xy} for samples with a Hall bar geometry and ohmic contacts as used in normal quasi-dc investigations of the quantum Hall effect. This work is stimulated by the theoretical paper of Christen and Büttiker,[14] who calculated the low-frequency admittance of quantized Hall conductors using an edge-state formalism. Section II deals with the frequency dependence of the longitudinal and the Hall impedances. We fit the longitudinal impedance versus frequency using the characteristic equation of a parallel LCR circuit. In this model, which is valid for all filling factors we show that the inductance scales as $1/\nu^2$ and the resistance as $1/\nu$. The Hall impedance is shown to decrease with increasing frequency, and in the low-frequency regime this decrease depends quadratically on the frequency and scales as $1/\nu^3$. In Sec. III we recall the approximated expressions of $Z_{xx}(\omega)$ and $Z_{xy}(\omega)$ developed by Christen and Büttiker and discuss the limit of the validity of these equations by comparison with the experimental data. In the edge-state picture the physical origin of the inductive behavior of the longitudinal impedance is well explained by the capacitive coupling between edge channels. Keeping higher-order terms leads to generalized equations of which the LCR model is an approximation. The theory of Christen and Büttiker successfully predicts the observed scaling of the equivalent-circuit parameters, both for the longitudinal and the Hall impedances. Finally, in Sec. IV we show results for a four-terminal cross sample for which all possible permutations of contacts and magnetic field direction have been measured. The large asymmetry in the equivalent-circuit parameters observed when inverting the magnetic field or inverting the current contacts can be understood when the direction of propagation of the edge states is taken into account.

II. FREQUENCY MEASUREMENTS

For the investigation a number of GaAs/(Al,Ga)As modulation-doped heterojunction (HJ) and single-quantum-well (QW) structures were grown by molecular beam epitaxy. We present results for two samples but stress that qualitatively similar frequency dependences have been obtained

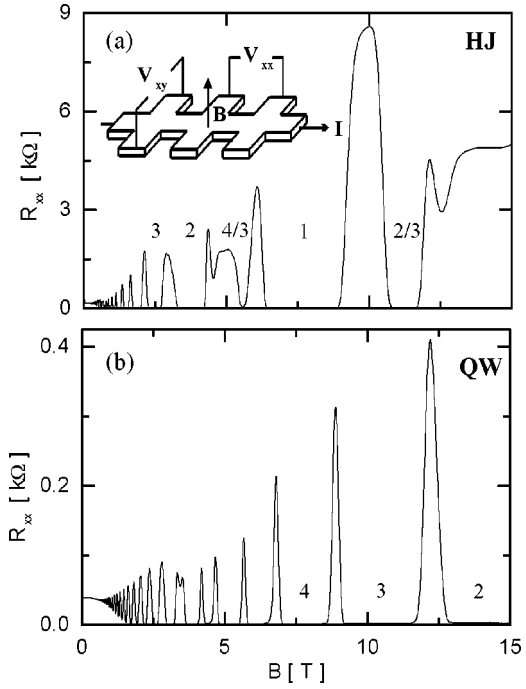

FIG. 1. Magnetoresistance trace measured at $T=50$ mK and under quasi-dc conditions ($I=100$ nA at 10.7 Hz) for (a) the HJ sample and (b) the QW sample. The inset shows a schematic of the Hall bar geometry used.

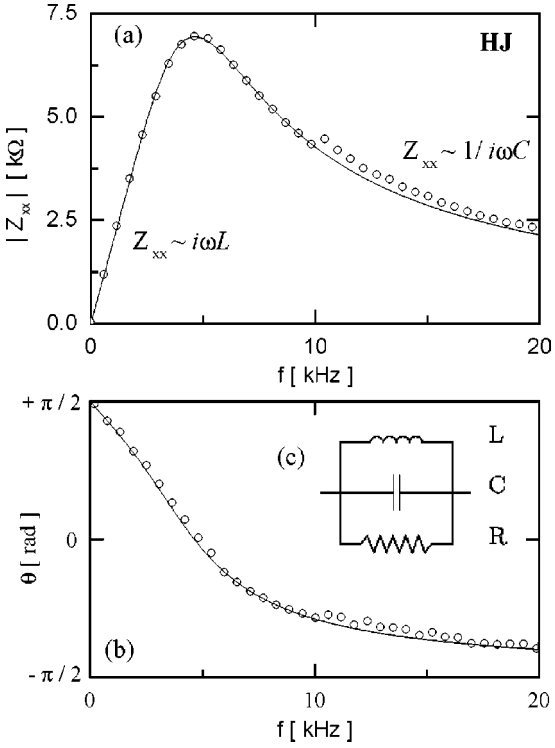

FIG. 2. (a) Magnitude of the longitudinal impedance $|Z_{xx}|$ versus frequency at $\nu=1$ for the HJ sample measured at $T=50$ mK. The solid line is the predicted frequency dependence of the magnitude of the impedance for the equivalent parallel LCR circuit with $L=314$ mH, $R=6.94$ kΩ, and $C=3.75$ nF as described in the text. (b) Frequency dependence of the measured phase. The solid line is the predicted phase for the equivalent LCR circuit. (c) Schematic of the equivalent LCR circuit.

on a number of both electron and hole 2D systems. The HJ sample has a carrier density of 1.35×10^{11} cm^{-2} with a mobility of 36 m^2 V^{-1} s^{-1}. The QW sample has a well width of 8.2 nm and a carrier density of 7.5×10^{11} cm^{-2} with a mobility of 11 m^2 V^{-1} s^{-1}. Hall bars were patterned to have a width $d=250$ μm with 750 μm between voltage probes. The geometry is indicated schematically in the inset of Fig. 1. Typical magnetoresistance traces measured at 50 mK and under quasi-dc conditions (10.7 Hz) with a current of 100 nA are shown in Fig. 1 for the HJ and QW sample. Millikelvin temperatures are used in order to have the maximum number of filling factors in a dissipationless state and for the HJ sample to have access to fractional filling factors. Such low temperatures are, however, not essential as the quantitative form of frequency dependence turns out to be almost temperature independent, provided the temperature is sufficiently low so that the conductance is almost dissipationless under quasi-dc conditions.

We begin by presenting results for the HJ sample. Figure 2(a) shows the frequency dependence of the modulus of the longitudinal impedance $|Z_{xx}|$ for $\nu=1$. For the study an EG&G 5210 lock-in amplifier was used with the $R\theta$ option, which allows to simultaneously measure the magnitude of the impedance and the phase. The ac current used was 100 nA at all frequencies. The impedance $|Z_{xx}|$ increases linearly from zero at low frequencies, and reaches a maximum before decreasing at higher frequencies. This form of the frequency dependence is reminiscent of a driven simple harmonic oscillator with strong damping, the electrical equivalent of which is a parallel LCR circuit, which is shown schematically in Fig. 2(c). The complex impedance of such a circuit is given by

$$Z_{xx}(\omega)=\frac{j\omega L}{1+j\omega L/R-\omega^2 CL}, \tag{1}$$

where $\omega=2\pi f$ is the angular frequency. In the low-frequency linear regime the longitudinal impedance is purely inductive and can be approximated by $Z_{xx}=2\pi fL$. From the slope $d|Z_{xx}|/df$ it is possible to extract the value of the inductance $L=314$ mH of the equivalent LCR circuit. Resonance occurs when $\omega^2CL=1$, conditions under which the impedance is purely resistive. The maximum of $|Z_{xx}|$ therefore allows us to deduce the value of the resistance $R=6.94$ kΩ. At high frequencies it is the capacitance that dominates and the equivalent capacitance $C=3.75$ nF can be deduced from the $1/\omega C$ decrease. The solid line in Fig. 2(a) is the characteristic of the equivalent parallel LCR circuit, and the agreement with the experimental data is good, in particular the circuit parameters correctly predict the observed resonance frequency. The validity of the LCR model is further confirmed by the measured phase of the voltage with respect to the injected current shown in Fig. 2(b). At low frequency the voltage leads the current by $+\pi/2$ as expected for an inductive behavior. As the frequency is increased the phase decreases, passing through zero on resonance before saturating at a value of $-\pi/2$ at high frequency where the impedance is dominated by the capacitance. The solid line is the predicted phase for the LCR circuit model, i.e.,

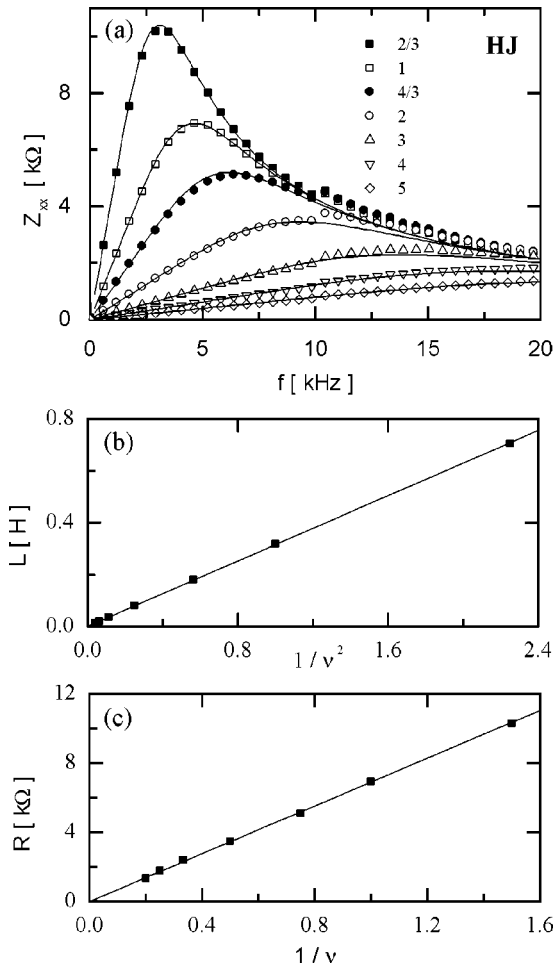

FIG. 3. (a) Magnitude of the longitudinal impedance as a function of frequency for even, odd, and fractional filling factors measured for the HJ sample measured at $T=50$ mK. The solid lines have been generated using Eq. (3) with $L_0=314$ mH, $R_0=6.94$ kΩ, and $C_0=3.75$ nF. (b) The measured equivalent inductance L versus inverse filling factor squared. The solid line is a least squares fit to the data. (c) The measured equivalent resistance R as a function of the inverse filling factor.

$$\theta=\arctan[R(1-\omega^2CL)/\omega L], \tag{2}$$

calculated using the previously determined values or L, C, and R.

Having demonstrated the validity of the LCR equivalent-circuit model for the case of $\nu=1$ we now turn our attention to other filling factors. The measured frequency dependence of the longitudinal impedance is shown in Fig. 3(a) for both odd, $\nu=1,3,5$, even, $\nu=2,4$, and fractional $\nu=2/3,4/3$ filling factors. Other filling factors are either not dissipationless under quasi-dc conditions or out of field range ($\nu=1/3$). All the curves present a similar shape with a linear regime at low frequencies, a maximum at the resonance and a decrease at high frequency. However, the parameters of the equivalent LCR circuit model are obviously filling-factor dependent. As for filling factor $\nu=1$ we have determined the values L, C, and R for each filling factor. As can be seen from Fig. 3(b), which plots the measured inductance as a function of inverse filling factor squared, a remarkably simple scaling law exists with $L(\nu)=L_0/\nu^2$. A least-squares fit to the data gives a slope $L_0=314$ mH. The very similar value of the measured impedance for all filling factors at high frequencies suggests that the equivalent-circuit capacitance, $C_0\simeq 3.75$ nF, is independent of filling factor. The equivalent-circuit resistance for each filling factor, $R(\nu)$, can be determined directly from the impedance at resonance. A plot of the impedance on resonance versus $1/\nu$ [Fig. 3(c)] reveals that $R(\nu)$ shifts linearly with inverse filling factor according to $R(\nu)=R_0/\nu$ with $R_0=6.94$ kΩ. Incorporating the experimentally determined scaling into Eq. (1), a generalized expression for the magnitude of the impedance can be written

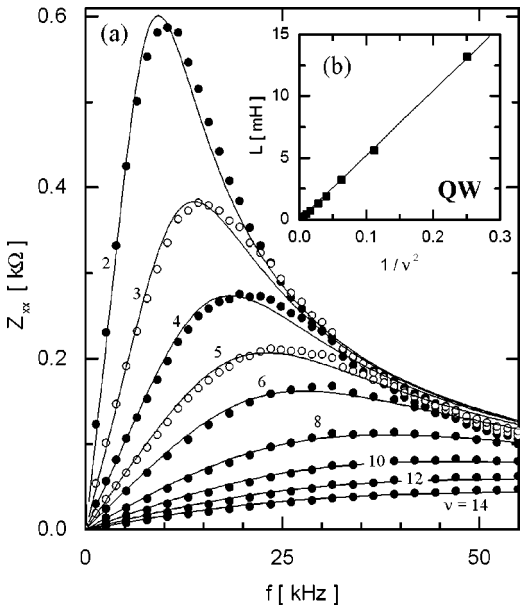

FIG. 4. (a) Magnitude of the longitudinal impedance as a function of frequency for even filling factors $\nu=2,4,\ldots,14$ (closed circles) and odd filling factors $\nu=3,5$ (open circles) for the QW sample measured at $T=50$ mK. The solid lines are calculated for the equivalent LCR circuit using Eq. (3) as described in the text. (b) The measured equivalent circuit inductance versus inverse filling factor squared. The solid line is a least-squares fit to the data, the slope of which gives $L_0=53$ mH.

$$|Z_{xx}(\omega,\nu)|^{-1}=\sqrt{\frac{1}{[R_0/\nu]^2}+\left[\omega C_0-\frac{1}{\omega L_0/\nu^2}\right]^2}. \tag{3}$$

The fits generated using Eq. (3) are indicated by the solid lines in Fig. 3(a). The good agreement for odd, even, and fractional filling factors is notable and appears to validate our analysis. The simple scaling law that is able to correctly predict the behavior for all filling factors suggests that the size of the gap in the density of states at the Fermi level plays no role in determining the equivalent-circuit parameters.

The frequency dependence of the longitudinal impedance for the QW sample at odd and even filling factors shown in Fig. 4(a) is qualitatively identical to the frequency dependence of the HJ sample. The equivalent-circuit parameters have been deduced for each filling factor and the $1/\nu^2$ dependence of $L(\nu)$ is shown in Fig. 4(b). The solid lines in Fig. 4(a) show the predicted behavior of the equivalent LCR circuit model that is computed using Eq. (3) with $L_0=52$ mH, $R_0=1.3$ kΩ, and $C_0\simeq 29$ nF. A good agreement

between experiment and the predictions of the equivalent-circuit model is observed for all filling factors. While the existence of a single scaling law for odd, even, and fractional filling factors is at first sight surprising given their very different nature, we will see in Sec. III that the scaling of the inductance with filling factor has its origin in the quantized Hall resistance and is thus independent of the size of the gap in the density of states at the Fermi energy.

We emphasize that qualitatively identical results have been obtained for all possible combinations of voltage contacts and for several samples of different mobilities and carrier densities. In all cases a good fit to an equivalent LCR circuit model with the same scaling between filling factors is observed. The characteristic values of L, C, and R can vary by approximately an order of magnitude for different contacts for the same sample and between samples. Inverting the magnetic field for a given pair of voltage contacts also typically leads to an order of magnitude change in the observed LCR parameters. There seems to be no systematic relation between the LCR fitting parameters obtained and the electrical characteristics (carrier density or mobility) of the sample. The measurements have been carried out in both a dilution refrigerator and in a variable temperature cryostat. The wiring of both systems is very different, notably the dilution refrigerator has a $\sim 200\ \Omega$ lead resistance in series with the sample (current and voltage probes). Nevertheless, the equivalent-circuit parameters determined for a given sample/voltage probe combination are identical in both systems, which indicates that they have an intrinsic, sample-related origin. A more detailed discussion of the symmetry relations when permuting current or voltage probes or inverting magnetic field direction can be found in Sec. IV.

We have also measured the frequency dependence of the Hall impedance Z_{xy} in the same frequency range. At very low frequency $Z_{xy}(\omega)$ is equal to the dc quantized resistance $h/\nu e^2$, but as the frequency is increased the Hall impedance decreases monotonically and tends to zero at high frequency. Hartland *et al.*[10] measured the frequency dependence of the difference $\Delta Z_{xy}(\omega)=|Z_{xy}(\omega)|-|Z_{xy}(0)|$ obtained by subtracting the dc component $|Z_{xy}(0)|$. They showed that in the frequency range 0–5 kHz, $\Delta Z_{xy}(\omega)$ increased quadratically with the frequency. In Fig. 5(a) $\Delta Z_{xy}(\omega)$ measured for the QW sample is plotted as a function of the frequency squared; we see that in the low-frequency regime $\Delta Z_{xy}(\omega)$ decreases linearly with f^2. In addition to the different sign for $d\Delta Z_{xy}(\omega)/d\omega^2$ the variation observed by Hartland and coworkers was also considerably smaller than that reported here. It is possible to measure the low-frequency slopes $d\Delta Z_{xy}(\omega)/d\omega^2$ and to plot them against the inverse filling factor. This is shown in Fig. 5(b) where $d|\Delta Z_{xy}(\omega)|/d\omega^2$ measured for the QW sample is plotted versus $1/\nu^3$. Note that a logarithmic scale for both axes has been used for clarity. The solid line drawn through the data points has a slope of 1, indicating that $d|\Delta Z_{xy}(\omega)|/d\omega^2$ scales as $1/\nu^3$ over more than two orders of magnitude. As we will see in Sec. III the scaling of $dZ_{xy}(\omega)/d\omega^2$ with $1/\nu^3$ is predicted by the theory of Christen and Büttiker.

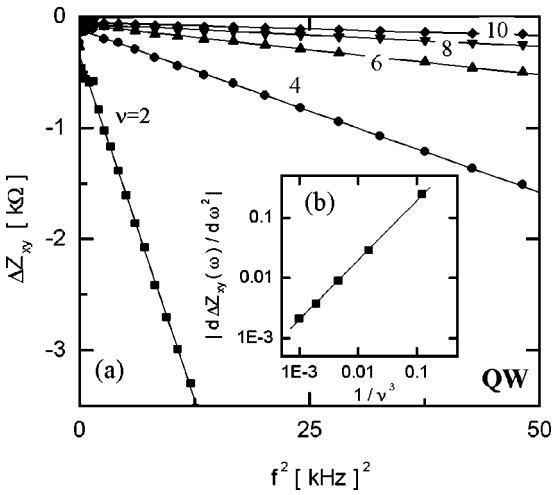

FIG. 5. (a) Variation of the magnitude of the Hall impedance $\Delta Z_{xy}(\omega)=|Z_{xy}(\omega)|-|Z_{xy}(0)|$ as a function of frequency squared for the QW sample for different filling factors measured at $T=50$ mK. The solid lines are least squares fits to the data, the slope of which is $d\Delta Z_{xy}(\omega)/d\omega^2$. (b) $|d\Delta Z_{xy}(\omega)/d\omega^2|$ determined from the low-frequency slopes in (a) versus inverse filling factor cubed and plotted on a log-log scale. The solid line through the data points has a slope of 1.

III. EXPRESSIONS FOR THE LONGITUDINAL AND HALL IMPEDANCES

In Sec. II we have seen that the frequency dependence of the longitudinal impedance is empirically well explained by an equivalent parallel LCR circuit. In this model an inductancelike term appears but it cannot be directly linked to a physical inductance in the 2DEG. This inductive behavior has already been predicted theoretically by Christen and Büttiker.[14] They studied the dynamic transport properties of a two-dimensional electron gas within the edge-state picture and calculated the low-frequency admittance of quantized Hall conductors. Here we recall the essential points of their theory. The work of Christen and Büttiker is based on the adaptation of the existing edge-state theory[15] dealing with the dc transport problem to the ac case.

If one considers an ideal four-terminal cross as represented in Fig. 6 with the current contacts k and l and the voltage probes, m and n, the resistance is given by[15]

$$R_{kl,mn}=\frac{G_{mk}G_{nl}-G_{ml}G_{nk}}{D_{kn}}, \tag{4}$$

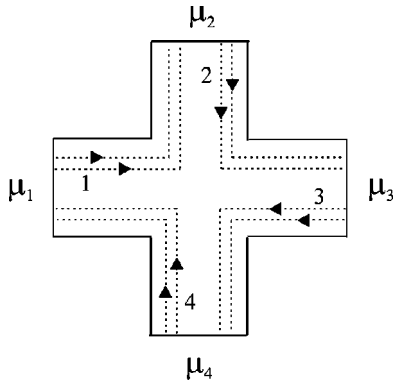

FIG. 6. Ideal four-terminal cross connecting electron reservoirs at electrochemical potential μ_i, $i=1,2,3,4$. The dashed lines represent the edge channels for the case $\nu=2$.

where the terms $G_{\alpha\beta}$ are the dc conductances and are expressed in terms of the quantized conductance $(\nu e^2)/h$ and D_{kn} is the 3×3 subdeterminant of the conductance matrix G with row k and column n omitted. In order to describe the ac transport in the 2DEG, capacitive terms have to be taken into account. This consideration leads to the notion of ac conductances (admittances) $G_{\alpha\beta}(\omega)$ that can be written as a development in ω terms up to the first[14] or second[16] order. By inserting these ac conductances in Eq. (4) one can calculate the expression of the low-frequency impedance $Z_{kl,mn}(\omega)$. Christen and Büttiker showed that for an ideal four-terminal cross the longitudinal and the Hall impedances can be written up to first order as follows:

$$Z_{xx}(\omega)=Z_{12,34}=j\omega\frac{c_{\mu,13}}{g^2}, \tag{5}$$

$$Z_{xy}(\omega)=Z_{13,24}=\frac{1}{g}+j\omega\frac{c_{\mu,24}-c_{\mu,13}}{g^2}, \tag{6}$$

where $g=(\nu e^2)/h$ is the quantized conductance at filling factor ν and $c_{\mu,kl}$ is the electrochemical capacitance between edge states k and l. We see that Eq. (5), which is an approximation including only terms up to first order and consequently only valid in the low-frequency range, predicts that $Z_{xx}(\omega)$ varies linearly with frequency and scales as $1/\nu^2$ in perfect agreement with our results. For the equivalent LCR circuit model the characteristic inductance can be written as $L_0=c_{\mu,13}(h/e^2)^2$. The physical origin of the inductive term in the Christen and Büttiker model can be simply understood as the capacitive coupling between the edge states associated with the current path and the edge states between the voltage contacts via the diagonal chemical capacitance $c_{\mu,13}$.

When invoking the predicted scaling $Z_{xx}(\omega)$ with $1/\nu^2$ we have implicitly assumed that the electrochemical capacitance is magnetic field independent. However, in the edge-state picture the electrochemical capacitance is given by $c_\mu^{-1}=c_0^{-1}+D_1^{-1}+D_2^{-1}$, where c_0 is the geometrical capacitance in series with the quantum capacitances D_1 and D_2.[14] This poses a number of problems; notably both the geometric and the quantum capacitances are predicted to be weakly magnetic field dependent while the simple $1/\nu^2$ scaling of $Z_{xx}(\omega)$ observed experimentally suggests that they are rigorously field independent. The microscopic description of the electrostatics of edge states is far from trivial[17] but a simple estimate of the size of the geometric capacitance gives $c_\mu\approx10^{-14}$ F, which is much smaller than the experimentally determined values of $c_\mu\approx10^{-10}$-10^{-12} F, corresponding to characteristic inductances $L_0\approx1-100$ mH. This suggests that something is either missing from the model or that the detailed microscopic picture of edge-state transport needs refining in order to obtain a quantitative agreement. It has been suggested[5] that the capacitive coupling can arise because of charge accumulation at the edge due to the Hall effect without invoking the presence of metallic edge channels. Furthermore, inductive imaging of the edge channels[13] have revealed that significant charge buildup can occur along one edge of the sample, the extent of which is too large to be consistent with the usual quantum-mechanical description of edge states.[17] However, the transmission formalism of Christen and Büttiker can be considered as quite general and therefore independent of the actual physical origin of the capacitances that couple the edges of the sample.

We now turn our attention to the frequency dependence of the magnitude of the Hall impedance. Both our results and those of Hartland and co-workers[10] show that $\Delta Z_{xy}(\omega)=|Z_{xy}(\omega)|-|Z_{xy}(0)|$ depends quadratically on the frequency, i.e., $\Delta Z_{xy}(\omega)\propto\omega^2$. From Eq. (6), $|Z_{xy}(\omega)|=\sqrt{1/g^2+\omega^2(c_{\mu,24}-c_{\mu,13})^2/g^4}$. Performing a Taylor expansion around $\omega=0$ gives $\Delta Z_{xy}(\omega)\approx\frac{1}{2}\omega^2(c_{\mu,24}-c_{\mu,13})^2/g^3$. Thus $|\Delta Z_{xy}(\omega)|$ is predicted to *increase* quadratically with frequency in agreement with the results of Hartland and co-workers[10] but in disagreement with the quadratic decrease shown in Fig. 5. However, for the case of an ideal four-terminal cross presenting a perfect symmetry the diagonal capacitances $c_{\mu,13}$ and $c_{\mu,24}$ are expected to be almost equal, suggesting that Eq. (6) should be modified to incorporate the higher-order terms.

Büttiker and Christen have expressed the equations of $Z_{xx}(\omega)$ and $Z_{xy}(\omega)$ up to the second order two[16] by writing the dynamical conductance $G_{\alpha\beta}(\omega)$ with a second-order term $K_{\alpha\beta}(\omega)$, which represents the charge relaxation. Here we propose to consider only first-order ac conductances but to retain the higher-order terms. The complex expressions for the longitudinal and the Hall impedances including all higher-order terms are given by[14]

$$Z_{xx}(\omega)=Z_{12,34}(\omega)=\frac{j\omega\alpha_1+\omega^2\alpha_2}{1+j\omega\alpha_3+\omega^2\alpha_4+j\omega^3\alpha_5} \tag{7}$$

and

$$Z_{xy}(\omega)=Z_{13,24}(\omega)=\frac{1/g+j\omega\beta_1+\omega^2\beta_2}{1+j\omega\beta_3+\omega^2\beta_4+j\omega^3\beta_5}, \tag{8}$$

where the coefficients α_i and β_i are combinations of the electrochemical capacitances $c_{\alpha\beta}$ (the μ subscript has been omitted for simplicity) and the quantized resistance $h/\nu e^2\equiv1/g$:

$$\alpha_1=c_{13}/g^2,\quad \beta_1=-[c_{11}+c_{33}]/g^2,$$

$$\alpha_2=[c_{12}c_{23}-c_{13}c_{22}]/g^3,\quad \beta_2=[c_{11}c_{33}-c_{13}^2]/g^3,$$

$$\alpha_3=\beta_3=[c_{11}+c_{12}+c_{13}+c_{22}+c_{23}+c_{33}]/g,$$

$$\alpha_4=\beta_4=[c_{12}^2+c_{13}^2+c_{23}^2+c_{13}(c_{12}+c_{23})-c_{33}(c_{12}+c_{22})$$

$$-c_{11}(c_{22}+c_{23}+c_{33})]/g^2,$$

$$\alpha_5=\beta_5=[c_{11}c_{23}^2+c_{22}c_{13}^2+c_{33}c_{12}^2-c_{11}c_{22}c_{33}$$

$$-2c_{12}c_{13}c_{23}]/g^3.$$

Comparing Eqs. (1) and (7) we see that the equivalent LCR circuit model and the Christen and Büttiker model are formally identical provided that $\alpha_2=\alpha_5=0$. In addition the predicted scaling of L, C, and R is in agreement with experiment. Comparing equivalent terms we see that the induc-

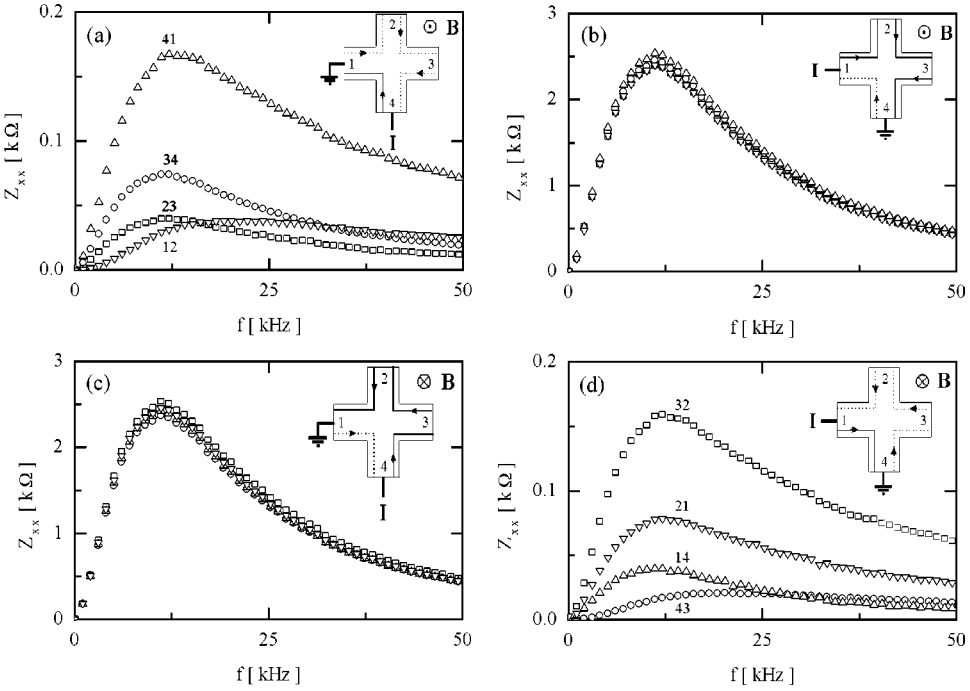

FIG. 7. Longitudinal impedance as a function of the frequency measured at $T=1.5$ K for (a) and (b) a positive magnetic field and (c) and (d) a negative magnetic field. Panels (a),(b) and (c),(d) differ in the relative position of source and sink (ground) current contacts as illustrated for the schematic cross in the inset of each figure. For each configuration $|Z_{xx}|$ has been measured for all four possible positions for the sink current contact. The pair of current contacts used is denoted by the different symbols as follows 12 or 21 (∇), 23 or 32 ($\square$), 34 or 43 ($\bigcirc$), 41 or 14 ($\triangle$).

tance $L \equiv \alpha_1 \propto 1/\nu^2$, the resistance $R \equiv \alpha_1/\alpha_3 \propto 1/\nu$, and the capacitance $C \equiv -\alpha_4/\alpha_1$ is independent of filling factor.

Taking the magnitude of the Hall impedance and performing a Taylor expansion around $\omega=0$, we obtain after some algebra an expression of the form

$$|Z_{xy}(\omega)| = 1/g - \frac{\gamma}{g^3}\omega^2 + \theta(\omega^4),$$

where γ has the dimensions of capacitance squared. This demonstrates that when all terms are included the Hall impedance is predicted to vary quadratically at low frequencies in agreement with experiment. In addition the model also correctly predicts the experimentally observed scaling of the low-frequency Hall impedance $d\Delta Z_{xy}(\omega)/d\omega^2 \propto 1/\nu^3$ shown in Fig. 5. As γ is a complicated combination of the sums and differences of the capacitance terms of the form $c_{kl}c_{mn}$ $(k,l,m,n=1,2,3,4)$ it is not possible to determine unambiguously from a theoretical viewpoint the sign of γ. We speculate that depending on the values of the sample specific electrochemical capacitances γ can be either positive or negative, which would explain the different signs for $d\Delta Z_{xy}(\omega)/d\omega^2$ observed by Hartland and co-workers and ourselves.

Here we propose to explain how Eq. (5), which results from the edge-state-based theory, could be found more intuitively by assuming the local picture of electronic transport. Let consider a 2DEG with a dc current I_x flowing along the x axis and a magnetic field B_z applied perpendicular to the electron plane. A Hall electric field E_H appears along the y direction, resulting in the accumulation of static charges at the edges. The injection of an ac current in the sample leads to an oscillating Hall electric field whose direction changes periodically and induces a dynamic transport of charges from one edge to the other. In this capacitorlike behavior the resulting displacement current can be written in the general form $I_y(\omega) = -i\omega C V_y(\omega)$. Finally the dynamic transport in the 2DEG can be viewed as a mixing of the transverse and the longitudinal Hall voltages due to $I_x(\omega)$ and $I_y(\omega)$, respectively, via the capacitive coupling. This consideration leads to the expression $V_x(\omega) = i\omega C(h/\nu e^2)^2 I_x(\omega)$, which confirms the prediction that $Z_{xx}(\omega)$ is proportional to the quantized resistance squared at low frequency.

IV. SYMMETRY CONSIDERATIONS

In order to investigate the symmetry relations when permuting voltage and current contacts we have fabricated samples with a four-terminal cross geometry from some of the remaining QW material. Each of the four arms of the cross were 250 μm wide and approximately 750 μm long. The carrier concentration and mobility for the cross samples are identical to that measured for the conventional QW Hall bar samples. The simple cross geometry facilitates the investigation of all different possible current and voltage probe configurations. We have verified that exchanging the voltage probes yields no change in the measured signal except the expected 180° phase change. It is therefore sufficient to consider the effect of different permutations of the current source and sink contacts. This is summarized in Fig. 7, which shows the longitudinal impedance for all possible permutations of current contacts in both positive and negative magnetic fields measured at filling factor $\nu=4$. All curves show the characteristic damped resonance consistent with an equivalent LCR circuit. In Fig. 7 two distinct cases are apparent: in (b) and (c) we observe almost identical curves with a large characteristic inductance and resistance while in (a) and (d) the curves are all different and the characteristic inductance and impedance are approximately an order of magnitude smaller. In addition the resonant frequency ($\approx$12 kHz) corresponding to the condition $\omega^2 LC=1$ is the same for all curves, which implies that the product LC is a constant. The observed symmetry can be qualitatively summarized as follows. Exchanging the source and sink for cur-

rent contacts or inverting the magnetic field changes the characteristics by an order of magnitude. Simultaneously exchanging the current contacts and inverting the magnetic field does not change the order of magnitude. Individual curves do, however, change as can most easily be seen when comparing Figs. 7(a) and 7(d). In particular it can be seen that Onsager-Casimir[18] reciprocity relation $Z_{kl,mn}(+B) = Z_{mn,kl}(-B)$ is obeyed.

This rather large asymmetry observed when exchanging the current source and the current sink is at first sight surprising, since the impedance is measured by applying an alternating current that continuously reverses direction. However, the symmetry of the problem is broken by the direction of the edge-state propagation, which is determined solely by the direction of the applied magnetic field and not the direction of the applied current. Although the Hall electric field in the bulk of the sample reverses when the current direction is reversed, the sign of the ''renormalized'' Hall electric field at the edge of the sample remains unchanged and hence the direction of propagation of the edge states remains unchanged. In the ac transport measurement the sink current contact is constantly at ground potential while the source contact oscillates between $\pm V$. Therefore, the edge state that leaves the sink contact is at ground potential while the edge state that leaves the source contact is at a potential $\pm V$. This is illustrated schematically in the insets of Fig. 7 where the edge state leaving the current source is shown as a solid line. This reasoning has been invoked[11] to explain why capacitance coefficients in multilead conductors are uneven under magnetic field reversal. Similar observations for electrons on the surface of liquid helium have also been explained in terms of the direction of propagation of edge magnetoplasmons.[4]

V. CONCLUSION

The frequency dependence of the longitudinal impedance of a two-dimensional electron gas at integer and fractional filling factors has been empirically shown to resemble that of a parallel LCR circuit. The parameters of the equivalent-circuit model scale with filling factor ν. The inductance scales as $1/\nu^2$, while the resistance scales as $1/\nu$ and the capacitance is independent of filling factor. The observation of an inductancelike behavior has been theoretically predicted by Christen and Büttiker,[14] who calculated the impedance by extending the transmission probability formalism to the ac case. When higher-order terms are retained a formal equivalence exists between theory and the LCR equivalent-circuit model. The theory also correctly predicts the observed scaling of L, C, and R with filling factor. The Hall impedance is found to vary quadratically with frequency as previously reported.[10] When higher-order terms are included the Christen-Büttiker model predicts a quadratic variation of the Hall impedance that scales as $1/\nu^3$ again in perfect agreement with experiment.

Even though the applicability of the edge-state picture over a wide range of experimental conditions seems doubtful, the transmission probability formalism[15] provides valuable insight into the dc quantum Hall effect and when extended to the ac case correctly predicts the frequency dependence of the impedance including the observed scaling with filling factor and therefore gives some theoretical basis for the empirically determined LCR equivalent-circuit model.

ACKNOWLEDGMENTS

We are grateful to M. Büttiker for a critical reading of the mansucript and useful discussions.

[1] K. von Klitzing, G. Dorda, and M. Pepper, Phys. Rev. Lett. **45**, 494 (1980).
[2] D. Tsui, H. L. Störmer, and A. C. Gossard, Phys. Rev. Lett. **48**, 1559 (1982).
[3] V. I. Talyanskii, A. V. Polisski, D. D. Arnone, M. Pepper, C. G. Smith, D. A. Ritchie, J. E. Frost, and G. A. C. Jones, Phys. Rev. B **46**, 12 427 (1992).
[4] P. K. H. Sommerfeld, R. W. van der Heijden, and F. M. Peters, Phys. Rev. B **53**, R13 250 (1996).
[5] A. M. C. Valkering, P. K. H. Sommerfeld, R. A. M. van der Ven, R. W. van der Heijden, F. A. P. Blom, M. J. Lea, and F. M. Peters, Phys. Rev. Lett. **81**, 5398 (1998).
[6] N. Q. Balaban, U. Meirav, H. Shtrikman, and V. Umansky, Phys. Rev. B **55**, R13 397 (1997).
[7] L. W. Engel, D. Shahar, C. Kurdak, and D. Tsui, Phys. Rev. Lett. **71**, 2638 (1993).
[8] R. Meisels, F. Kuchar, and K. Dybko, Ann. Phys. (Leipzig) **8**, 507 (1999).
[9] M. Pepper and J. Wakabayashi, J. Phys. C **16**, L113 (1983).
[10] A. Hartland, B. P. Kibble, P. J. Rodgers, and J. Bohacek, IEEE Trans. Instrum. Meas. **44**, 245 (1995).
[11] W. Chen, T. P. Smith III, M. Büttiker, and M. Shayegan, Phys. Rev. Lett. **73**, 146 (1994).
[12] S. Takaoka, K. Oto, H. Kurimoto, K. Murase, K. Gamo, and S. Nishi, Phys. Rev. Lett. **72**, 3080 (1994).
[13] E. Yahel, A. Tsukernik, A. Palevski, and H. Shtrikman, Phys. Rev. Lett. **81**, 5201 (1998).
[14] T. Christen and M. Büttiker, Phys. Rev. B **53**, 2064 (1996).
[15] M. Büttiker, Phys. Rev. Lett. **57**, 1761 (1986); Phys. Rev. B **38**, 9375 (1988); M. Büttiker, H. Thomas, and A. Prêtre, Phys. Lett. A **180**, 364 (1993); M. Büttiker, J. Phys.: Condens. Matter **5**, 9361 (1993).
[16] M. Büttiker and T. Christen, in *Proceedings of the International Conference on High Magnetic Fields in the Physics of Semiconductors II*, edited by G. Landwehr and W. Ossau (World Scientific, Singapore, 1997), p. 193; T. Christen and M. Büttiker, Phys. Rev. B **55**, R1946 (1997).
[17] D. B. Chklovskii, B. I. Shklovskii, and L. I. Glazman, Phys. Rev. B **46**, 4026 (1992).
[18] L. Onsager, Phys. Rev. **38**, 2265 (1931); H. B. G. Casimir, Rev. Mod. Phys. **17**, 343 (1945).